Electronic Supplementary Material (ESI) for Journal of Materials Chemistry C.

Supporting information

Decisive Role of Heavy-Atom Orientation for Efficient Enhancement of Spin-Orbit Coupling in Organic Thermally Activated Delayed Fluorescence Emitters

Michał Mońka,[1] Daria Grzywacz,[2] Estera Hoffman,[1] Vladyslav Ievtukhov,[2] Karol Kozakiewicz,[2] Radoslaw Rogowski,[1] Aleksander Kubicki,[1] Beata Liberek,[2] Piotr Bojarski,[1] Illia E. Serdiuk[1]*

[1] Faculty of Mathematics, Physics and Informatics, University of Gdańsk, Wita Stwosza 57, 80-308 Gdańsk, Poland

[2] Faculty of Chemistry, University of Gdańsk, Wita Stwosza 63, 80-308 Gdańsk, Poland

*Corresponding author. E-mail: illia.serdiuk@ug.edu.pl, phone + 48 58 523 22 44

Table of contents

Section S1: Photophysical measurements

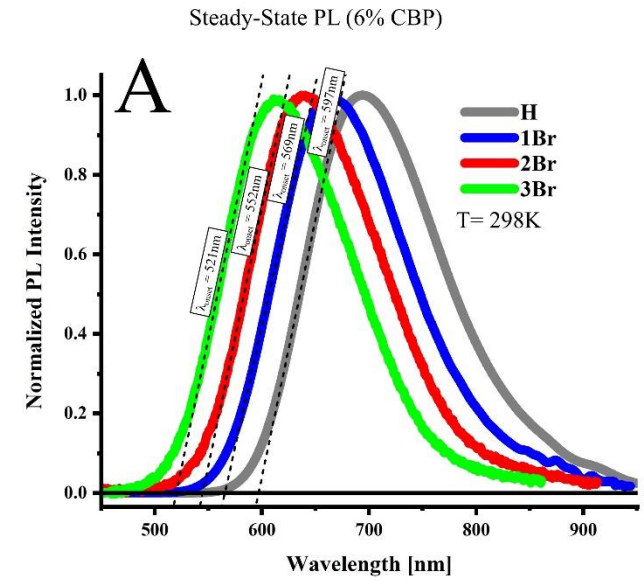

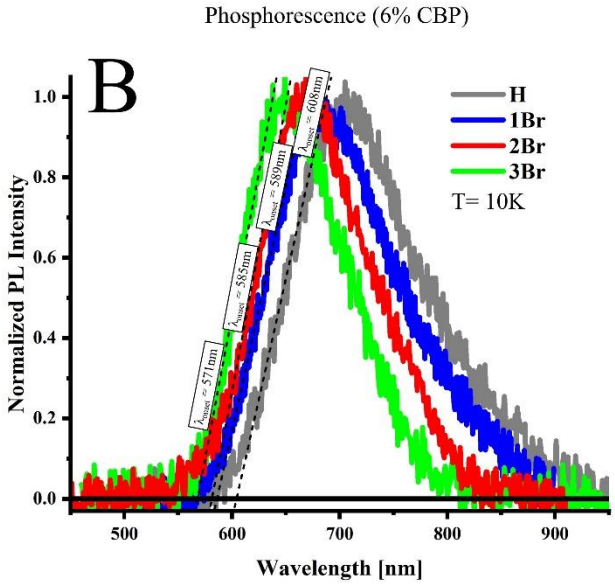

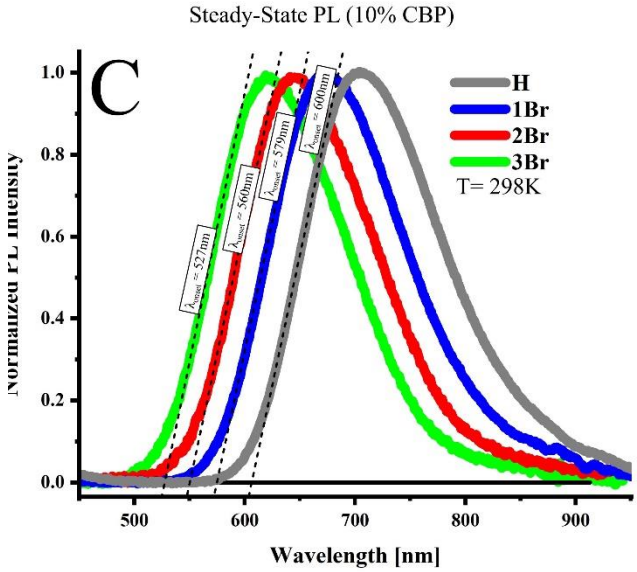

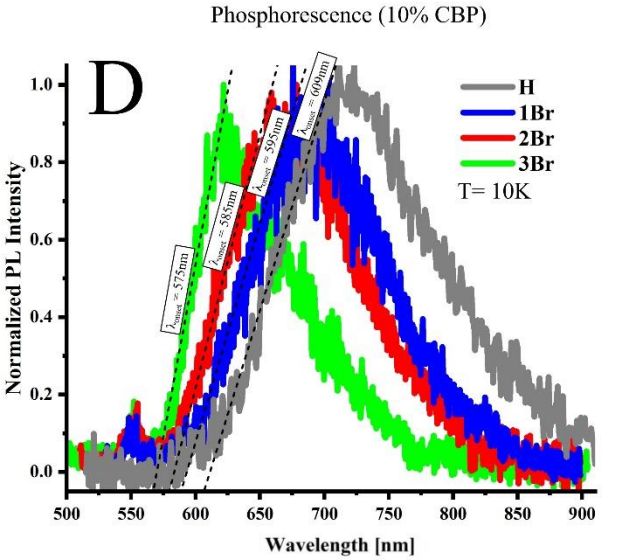

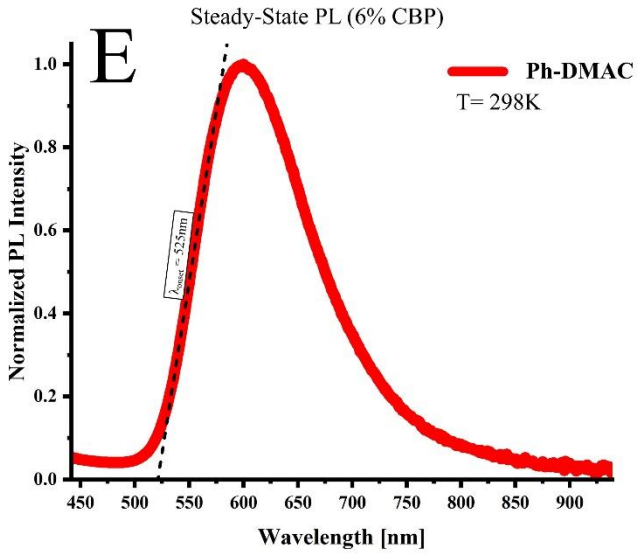

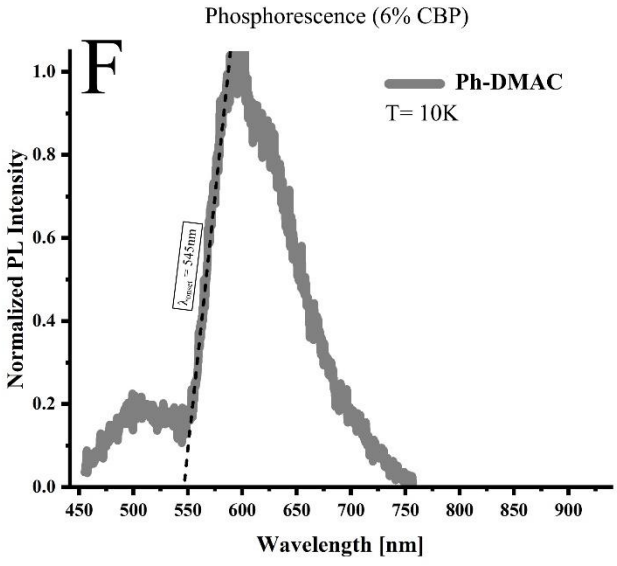

Figure S1. Steady-State PL spectra of investigated compounds: 6% (A, E) and 10% (C) CBP with onsets and phosphorescence spectra measured in 10K, 6% (B, F) and 10% (D) CBP.

Table S1. Experimental determination of ^{1}CT, ^{3}CT and ^{3}LE - onset values.

		Fluorescence		Phosphorescence			Phosphorescence			
	$w_{X/CBP}$	λ_{onset}	^{1}CT energy	λ_{onset}	^{3}CT energy	$\Delta E_{1CT-3CT}$		λ_{onset}	^{3}LE energy	$\Delta E_{1CT-3LE}$
		[nm]	[eV]	[nm]	[eV]	[eV]		[nm]	[eV]	[eV]
H	6%	597	2.07	608	2.04	0.04		552	2.25	-0.18
	10%	600	2.07	609	2.04	0.03				
1Br	6%	569	2.18	589	2.10	0.08	**ZNX** 0.1%	552	2.25	-0.07
	10%	579	2.14	595	2.08	0.06				
2Br	6%	552	2.25	585	2.12	0.13		552	2.25	0.00
	10%	560	2.21	585	2.11	0.10				
3Br	6%	521	2.37	571	2.17	0.20		552	2.25	0.13
	10%	527	2.35	575	2.16	0.19				

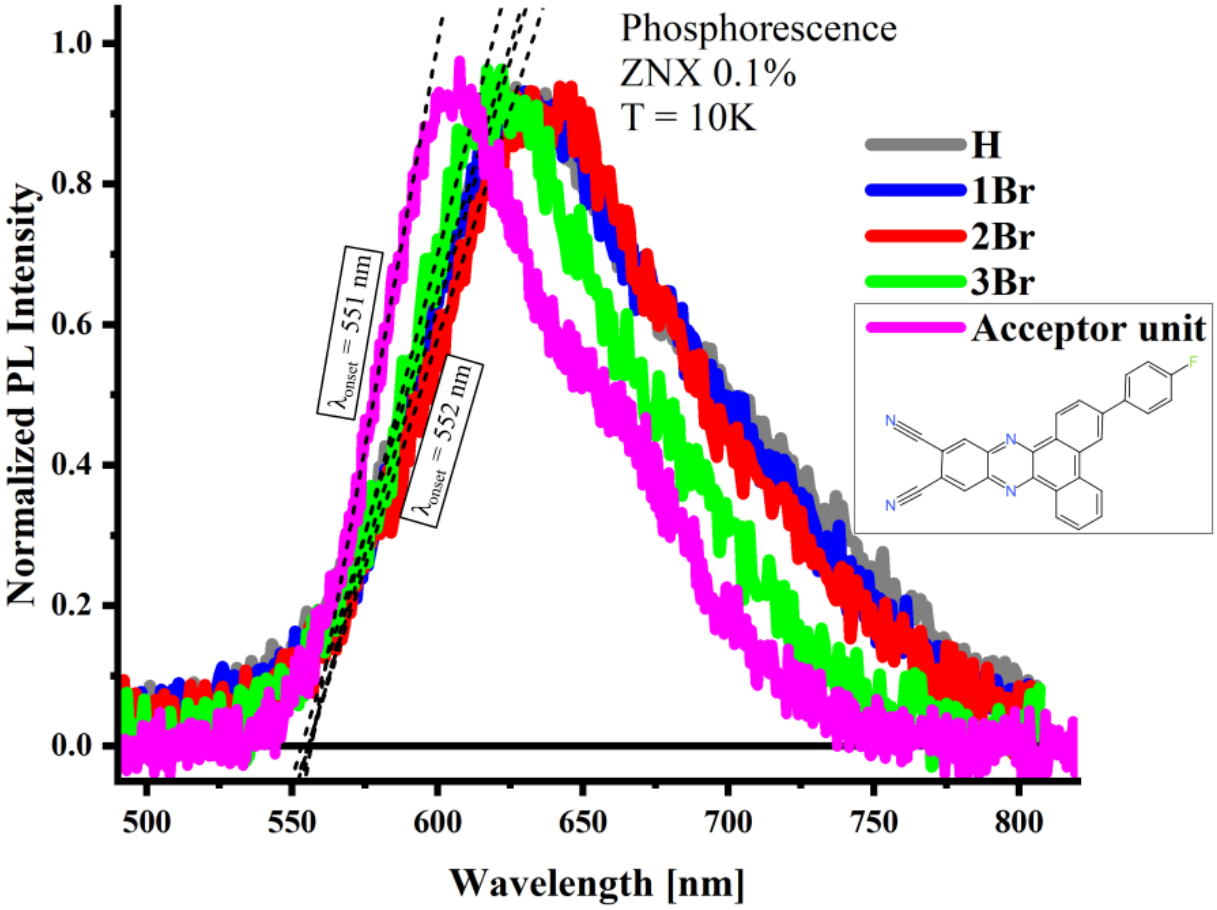

Figure S2. Phosphorescence spectra of investigated compounds dispersed in ZNX, measured in 10K under excitation wavelength λ_{exc} = 370 nm with a 20ms delay after excitation pulse.

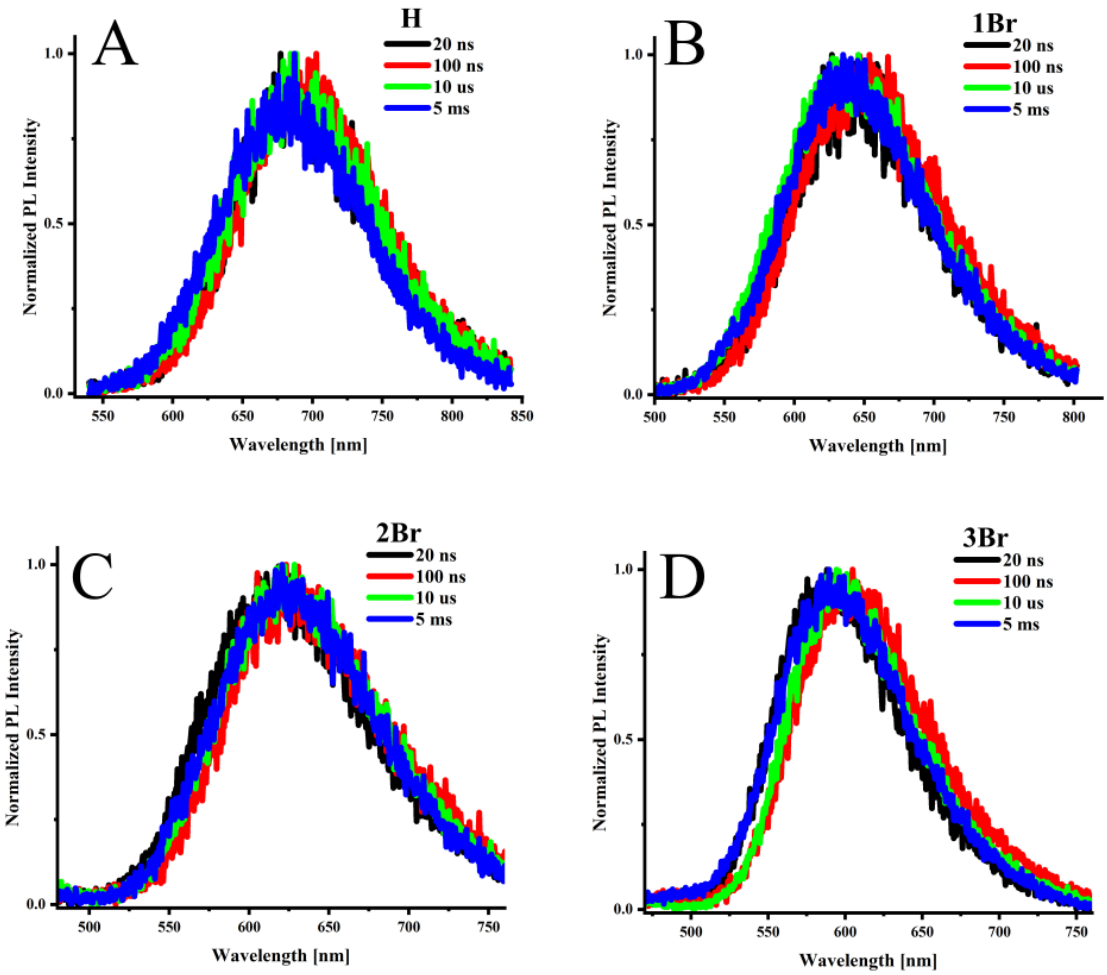

Figure S3. PL spectra of **H** (A), **1Br** (B), **2Br** (C), and **3Br** (D) in 6% CBP, taken at different time delays.

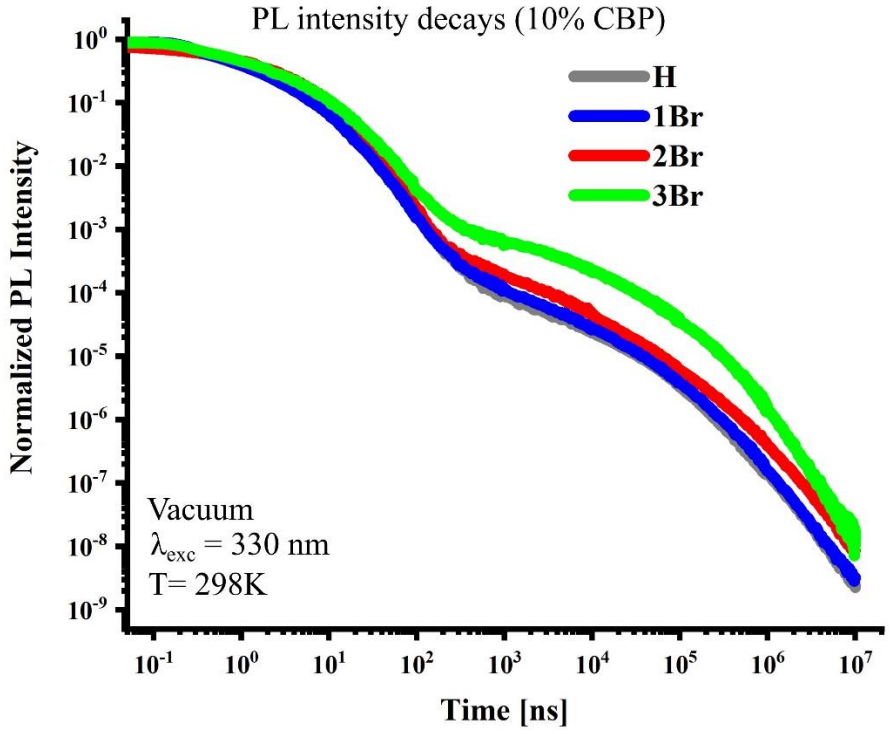

Figure S4. PL intensity decays of investigated compounds (10% CBP) measured in vacuum under excitation wavelength λ_{exc} = 330 nm.

Section S2: Quantum chemical calculations

Theoretical rate constants of rISC were calculated using Marcus-Hush equation:

$$k_{(r)ISC} = \frac{V^2}{\hbar}\sqrt{\frac{\pi}{k_B T\lambda}}\exp\left[-\frac{(\Delta E_{ST} + \lambda)^2}{4k_B T\lambda}\right], \quad \text{(S1)}$$

where V is SOC constant, $\hbar$ is reduced Planck constant, λ is sum of internal λ_{int} and external (λ_{solv}) reorganization energies for respective transition (in our calculations we assumed λ_{solv}, = 0.3 eV) ΔE_{ST} is the energy gap between singlet and respective triplet state, k_B stands for Boltzmann constant, T is temperature.

Relative contribution of *i*-th rotamers in **H**, **1Br**, **2Br** and **3Br**-rotamers was calculated using Boltzmann distribution law:

$$\mu_i[\%] = \frac{\exp\left(-\frac{\Delta E_i}{k_B T}\right)}{\sum_{i=1}^{N}\exp\left(-\frac{\Delta E_i}{k_B T}\right)}, \quad \text{(S2)}$$

where N is the number of existing isomers (for **H**, **1Br 2Br** and **3Br**-rotamers N = 2, 16, 16 and 32, respectively), ΔE_i denotes the energy difference between *i*-th rotamer and most stable rotamer (with lowest energy). Procedure for theoretical prediction rate constants described in details in [1].

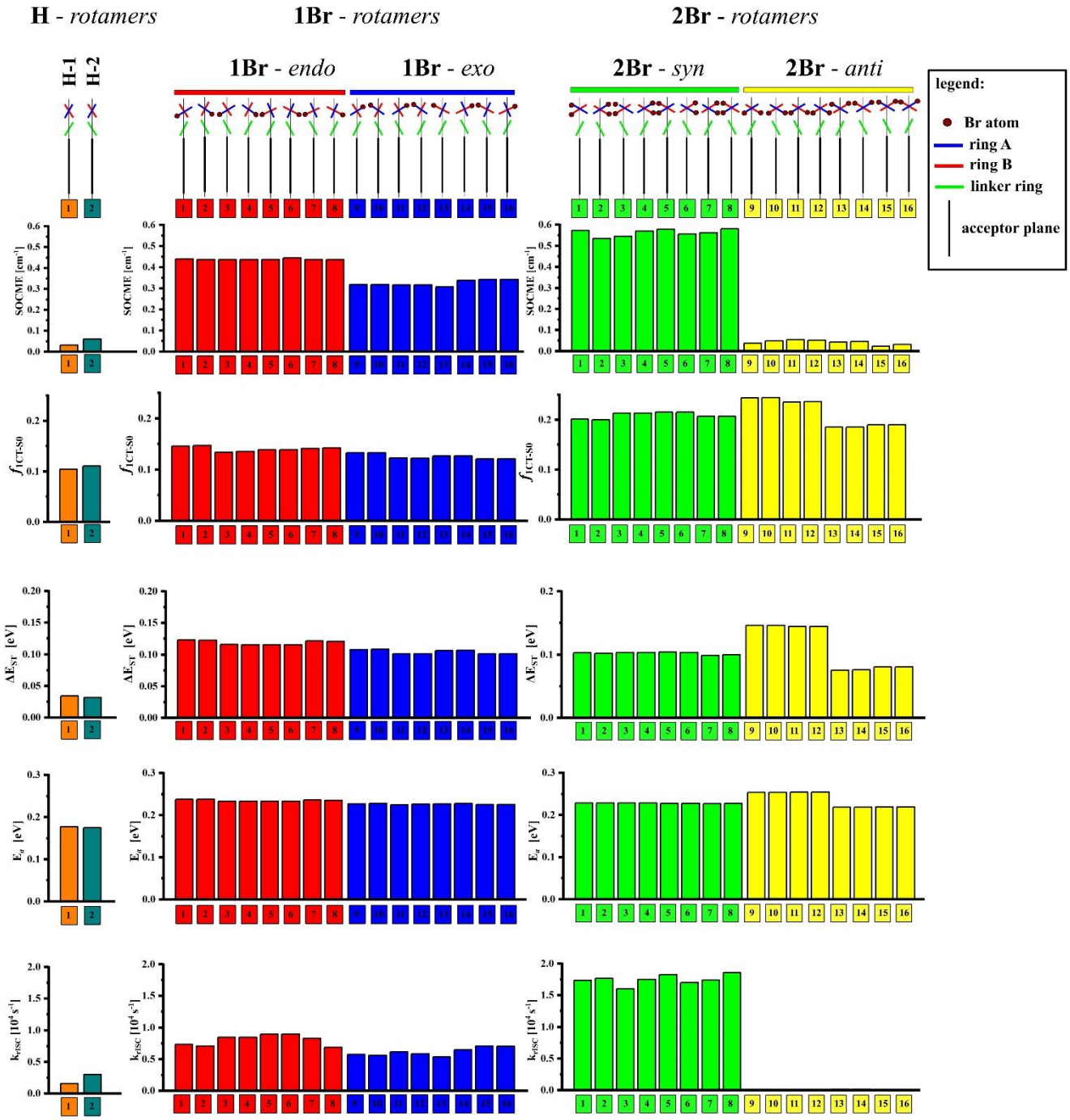

Figure S5. Calculated electronic parameters of all **H**, **1Br** and **2Br** – rotamers. In main text, key rotamers (depicted in **Figure 5**, **Table 3**) from each group: **H**-*rotamers*: **1** (as **H-1**) and **2** (as **H-2**); **1Br**-*rotamers:* **3** (as **1Br**-*endo*) and **12** (as **1Br**-*exo*); **2Br**-*rotamers*: **5** (as **2Br**-*syn*) and **9** (as **2Br**-*anti*).

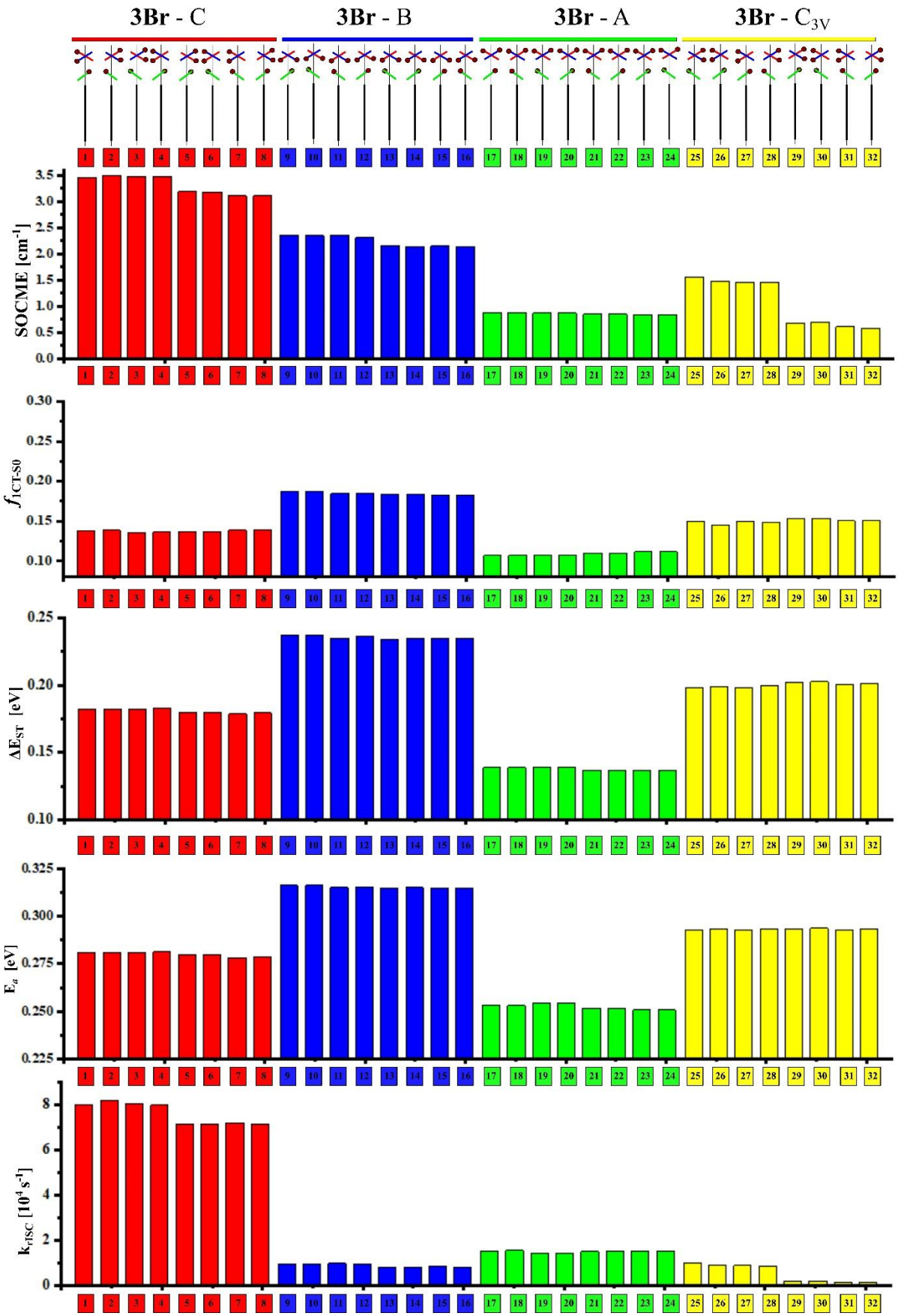

Figure S6. Calculated electronic parameters of all **3Br** rotamers. In main text, key rotamers (depicted in **Figure 5**, **Table 3**) from 3Br-rotamers group: **32** (as **3Br**-C_{3V}), **17** (as **3Br**-A), **21** (as **3Br**-A), **12** (as **3Br**-B), **1** (as **3Br**-C).

Table S2. Calculated values of different geometry (dihedrals θ_L, θ_A, and θ_B) and electronic parameters (plotted in **Figures S5** and **S6**) of all rotamers.

H - *rotamers*	**1**	**2**	**X**[a]
$SOC_{T1\text{-}S1}$ [cm^{-1}]	0.06	0.08	--
$\Delta E_{3CT\text{-}1CT}$ [eV]	0.03	0.03	**0.03**
$f_{S1\text{-}S0}$	0.10	0.11	**0.107**
E_a [eV]	0.18	0.17	--
μ [%]	67.2	32.8	--
k_{rISC} [10^4 s^{-1}]	0.16	0.30	**0.20**
θ_L	27.9	-28.8	
θ_A	-64.6	-65.1	
θ_B	-64.8	-65.2	

1Br- *rotamers*	**1**	**2**	**3**	**4**	**5**	**6**	**7**	**8**	**9**	**10**	**11**	**12**	**13**	**14**	**15**	**16**	**X**[a]
$SOC_{T1\text{-}S1}$ [cm^{-1}]	0.44	0.43	0.44	0.44	0.44	0.44	0.45	0.41	0.32	0.32	0.32	0.32	0.31	0.34	0.34	0.34	--
$\Delta E_{3CT\text{-}1CT}$ [eV]	0.12	0.12	0.12	0.12	0.12	0.12	0.12	0.12	0.11	0.11	0.10	0.10	0.11	0.11	0.10	0.10	**0.11**
$f_{S1\text{-}S0}$	0.15	0.15	0.13	0.14	0.14	0.14	0.14	0.14	0.13	0.13	0.12	0.12	0.13	0.13	0.12	0.12	**0.131**
E_a [eV]	0.24	0.24	0.23	0.23	0.23	0.23	0.24	0.24	0.23	0.23	0.22	0.23	0.23	0.23	0.23	0.23	--
μ [%]	7.0	4.3	1.5	2.0	7.3	10.6	3.9	21.8	7.6	2.1	9.0	3.3	6.6	5.0	3.0	5.1	--
k_{rISC} [10^4 s^{-1}]	0.7	0.7	0.8	0.8	0.9	0.9	0.8	0.7	0.6	0.6	0.6	0.6	0.5	0.6	0.7	0.7	**0.71**
θ_L	21.3	-21.1	-22.6	22.5	22.3	-22.3	-22.6	22.7	23.2	-23.1	-23.0	22.4	23.6	-23.6	-21.9	21.9	
θ_A	-74.6	74.7	-74.9	74.9	56.0	-56.0	55.9	-55.9	69.2	-69.1	68.4	-68.8	-55.3	55.2	-55.3	55.2	
θ_B	-56.1	56.5	-56.1	56.2	75.1	-75.1	74.9	-74.9	-55.4	55.3	-55.3	55.1	69.5	-69.2	69.0	-68.8	

2Br- *rotamers*	**1**	**2**	**3**	**4**	**5**	**6**	**7**	**8**	**9**	**10**	**11**	**12**	**13**	**14**	**15**	**16**	**X**[a]
$SOC_{T1\text{-}S1}$ [cm^{-1}]	0.57	0.53	0.54	0.57	0.58	0.56	0.56	0.58	0.04	0.05	0.05	0.05	0.04	0.05	0.02	0.03	--
$\Delta E_{3CT\text{-}1CT}$ [eV]	0.10	0.10	0.10	0.10	0.10	0.10	0.10	0.10	0.15	0.15	0.14	0.14	0.08	0.08	0.08	0.08	**0.13**
$f_{S1\text{-}S0}$	0.20	0.20	0.21	0.21	0.22	0.22	0.21	0.21	0.24	0.24	0.24	0.24	0.19	0.19	0.19	0.19	**0.216**
E_a [eV]	0.23	0.23	0.23	0.23	0.23	0.23	0.23	0.23	0.25	0.25	0.25	0.25	0.22	0.22	0.22	0.22	--
μ [%]	0.8	3.3	1.1	1.1	7.2	1.5	1.6	5.0	12.1	8.3	27.5	27.8	1.0	0.8	0.4	0.4	--
k_{rISC} [10^4 s^{-1}]	1.7	1.8	1.6	1.8	1.8	1.7	1.7	1.9	0.0	0.0	0.0	0.0	0.0	0.0	0.0	0.0	**0.40**
θ_L	16.2	-16.1	-18.0	17.8	17.8	-17.9	-16.3	16.8	17.6	-17.7	-15.1	15.1	17.2	-17.1	-18.2	18.2	
θ_A	-77.5	77.5	-77.3	77.2	-63.5	63.5	-63.3	63.4	-68.5	68.5	-68.3	68.3	-78.4	78.2	-78.9	-68.7	
θ_B	63.3	-63.2	63.1	-63.2	77.3	-77.4	77.1	-77.1	-68.4	68.3	-68.3	68.3	-78.1	78.2	-78.4	78.4	

3Br- *rotamers*	**1**	**2**	**3**	**4**	**5**	**6**	**7**	**8**	**9**	**10**	**11**	**12**	**13**	**14**	**15**	**16**	**17**	**18**	**19**	**20**	**21**	**22**	**23**	**24**	**25**	**26**	**27**	**28**	**29**	**30**	**31**	**32**	**X**[a]
$SOC_{T1\text{-}S1}$ [cm^{-1}]	3.45	3.50	3.47	3.48	3.19	3.18	3.11	3.11	2.35	2.35	2.36	2.31	2.15	2.14	2.15	2.14	0.88	0.88	0.87	0.87	0.85	0.85	0.84	0.84	1.56	1.48	1.46	1.46	0.68	0.69	0.61	0.58	--
$\Delta E_{3CT\text{-}1CT}$ [eV]	0.18	0.18	0.18	0.18	0.18	0.18	0.18	0.18	0.24	0.24	0.24	0.24	0.23	0.23	0.23	0.23	0.14	0.14	0.14	0.14	0.14	0.14	0.14	0.14	0.20	0.20	0.20	0.20	0.20	0.20	0.20	0.20	**0.20**
$f_{S1\text{-}S0}$	0.14	0.14	0.14	0.14	0.14	0.14	0.14	0.14	0.19	0.19	0.18	0.19	0.18	0.18	0.18	0.18	0.11	0.11	0.11	0.11	0.11	0.11	0.11	0.11	0.15	0.15	0.15	0.15	0.15	0.15	0.15	0.15	**0.118**
E_a [eV]	0.28	0.28	0.28	0.28	0.28	0.28	0.28	0.28	0.32	0.32	0.32	0.32	0.31	0.32	0.31	0.31	0.25	0.25	0.25	0.25	0.25	0.25	0.25	0.25	0.29	0.29	0.29	0.29	0.29	0.29	0.29	0.29	--
μ [%]	6.90	0.92	2.12	1.97	1.12	0.95	2.49	2.67	2.18	2.18	3.86	4.14	4.63	4.61	14.68	2.94	0.41	0.46	0.74	0.67	0.56	1.96	0.70	0.65	4.13	3.48	3.53	3.57	5.66	10.15	2.73	2.24	--
k_{rISC} [10^4 s^{-1}]	8.0	8.2	8.0	8.0	7.1	7.1	7.2	7.1	0.9	0.9	1.0	0.9	0.8	0.8	0.8	0.8	1.5	1.6	1.4	1.5	1.5	1.5	1.5	1.5	1.0	0.9	0.9	0.2	0.2	0.2	0.2	0.1	**2.09**
θ_L	18.1	-18.2	17.5	-17.5	-16.9	16.9	-17.3	17.3	-16.6	16.6	-17.7	17.8	15.5	-15.5	15.7	-15.6	19.5	-19.7	17.5	-17.4	-18.0	18.0	-18.8	18.8	16.1	-15.8	14.5	-14.3	-17.7	17.6	-19.0	18.9	
θ_A	-71.0	71.0	61.2	-61.2	60.9	-60.9	-71.5	71.5	77.8	-77.8	77.8	-77.5	77.9	-77.9	78.0	-77.9	76.5	-76.4	-83.5	-61.8	75.9	-75.9	61.0	-61.0	75.4	-75.3	-75.8	75.9	75.1	-75.1	74.8	76.6	
θ_B	61.4	-61.3	-70.9	70.9	-71.4	71.4	60.9	-60.9	73.6	-73.6	73.6	-73.6	74.0	-74.0	74.0	-74.0	61.7	-61.7	76.8	-76.7	60.8	-60.8	75.5	-75.5	-75.7	75.7	75.2	-75.1	-76.2	76.3	-76.6	-74.8	

[a] – statistical mean values (weighted using Boltzmann distribution law - equation S2);
$SOC_{T1\text{-}S1}$ [cm^{-1}] – SOC constant value for 3CT →1CT transition;
$\Delta E_{3CT\text{-}1CT}$ [eV] – Energy gap between ^{3}CT and ^{1}CT excited states;
$f_{S1\text{-}S0}$ – oscillator strength;
E_a [eV] – Activation energy;
μ [%] – relative contribution estimated using Boltzmann distribution law - equation S2);
k_{rISC} [10^4 s^{-1}] – calculated rate constant for ^{3}CT →^{1}CT transition.
θ_L θ_A θ_B – dihedral angles (**Figure 3**)

Calculations of the ^{3}LE→^{1}CT rate constants. To verify whether ^{3}LE→^{1}CT channel has an impact on rISC, we performed theoretical calculations of its rate constants ($k_{3LE\text{-}1CT}$) using Marcus-Hush equation (S1) and experimental $\Delta E_{3LE\text{-}1CT}$ values. Since we consider two triplet states from which rISC is potentially possible, at first, we estimated relative population of these levels using Boltzmann distribution law:

$$\chi_i[\%] = \frac{\exp\left(-\frac{\Delta E_i}{k_B T}\right)}{\sum_{i=1}^{N} \exp\left(-\frac{\Delta E_i}{k_B T}\right)}, \quad \text{(S3)}$$

where ΔE_i denotes the energy difference between lowest triplet state (T_1) and respective triplet state (T_i):

$$\Delta E_i = (T_i - T_1), \quad \text{(S4)}$$

$$a_i = \exp\left(-\frac{(T_i - T_1)}{k_B T}\right). \quad \text{(S5)}$$

Table S3. Theoretical constant rates $k_{3LE\text{-}1CT}$ with determined population of lowest triplet excited states of emitters.

Alignment of triplet excited states:	CBP 10% T_2 = **^{3}LE(A)** T_1 = **^{3}CT**					**^{3}LE(A)**	**^{3}CT**		
	T_1	T_2	$\Delta E_{T2\text{-}T1}$	a_1	a_2	$\chi_{3LE(A)}$	χ_{3CT}	$k_{3LE\text{-}1CT}$	$\chi_{3LE(A)} k_{3LE\text{-}1CT}$
	[eV]	[eV]	[eV]			[%]	[%]	[10^4 s^{-1}]	**[10^4 s^{-1}]**
H	2.03	2.25	0.22	1	0.0003	0.03	99.97	186.2	**0.04**
1Br	2.08	2.25	0.17	1	0.0018	0.18	99.82	24.4	**0.03**
2Br	2.11	2.25	0.14	1	0.0070	0.70	99.30	1.1	**0.01**
3Br	2.16	2.25	0.09	1	0.0281	2.92	97.08	3.8	**0.10**

From the results included in Table S3, it can be seen, that population of triplet states is strongly dominated by ^{3}CT state due to large difference in energies between ^{3}CT and ^{3}LE levels.

Next, values of $k_{3LE\text{-}1CT}$ for each emitter were calculated just as $k_{3CT\text{-}1CT}$, taking into account population of ^{3}LE state $\chi_{3LE(A)}$. Results are presented in **Table S3** and **Figure 4.**

Since theoretical predictions of rISC constant rates based on exclusively ^{3}LE-^{1}CT channel did not showed a good correlation with experimental values, we conclude that ^{3}LE-^{1}CT channel has not considerable impact on rISC in most of the cases except for the rotamers with very low rates of ^{3}CT-^{1}CT transition as **2Br**-*anti* ones.

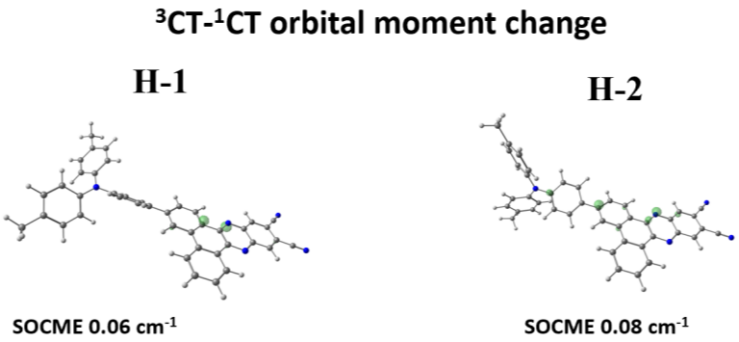

Figure S7. Differences in the orbital transition moment of **H** rotamers. **note that contour value is 0.01 (high)*

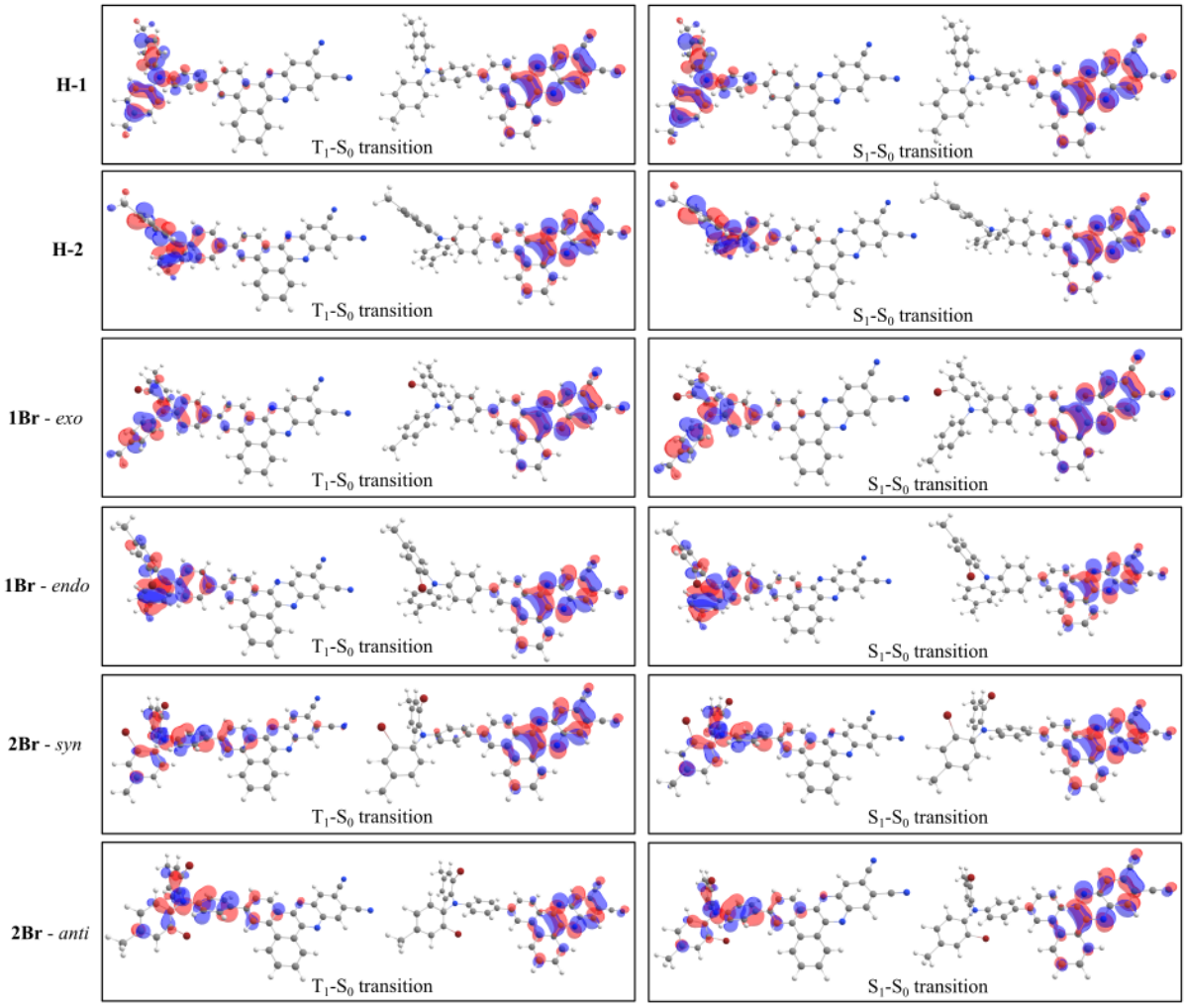

Figure S8. Natural transition orbitals for the S_1-S_0 and T_1-S_0 transitions for selected **H**, **1Br** and **2Br** rotamers. NTO indicate almost negligible role of bromine atoms in the electronic transitions.

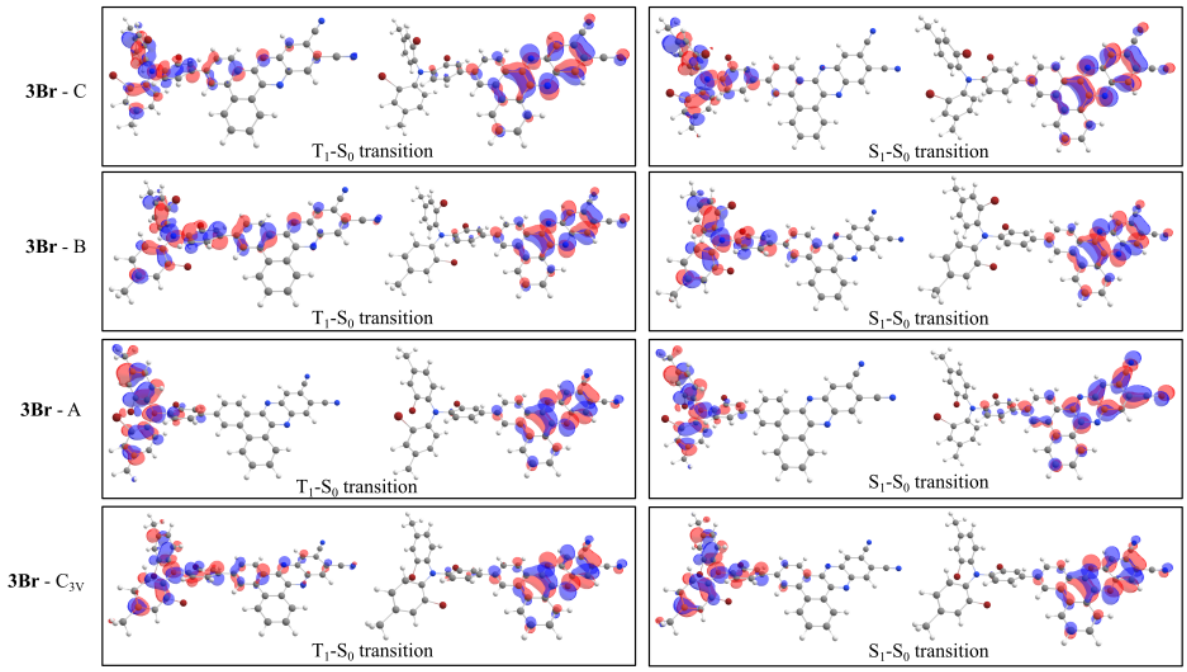

Figure S9. Natural transition orbitals for the S_1-S_0 and T_1-S_0 transitions for selected **3Br** rotamers. NTO indicate almost negligible role of bromine atoms in the electronic transitions.

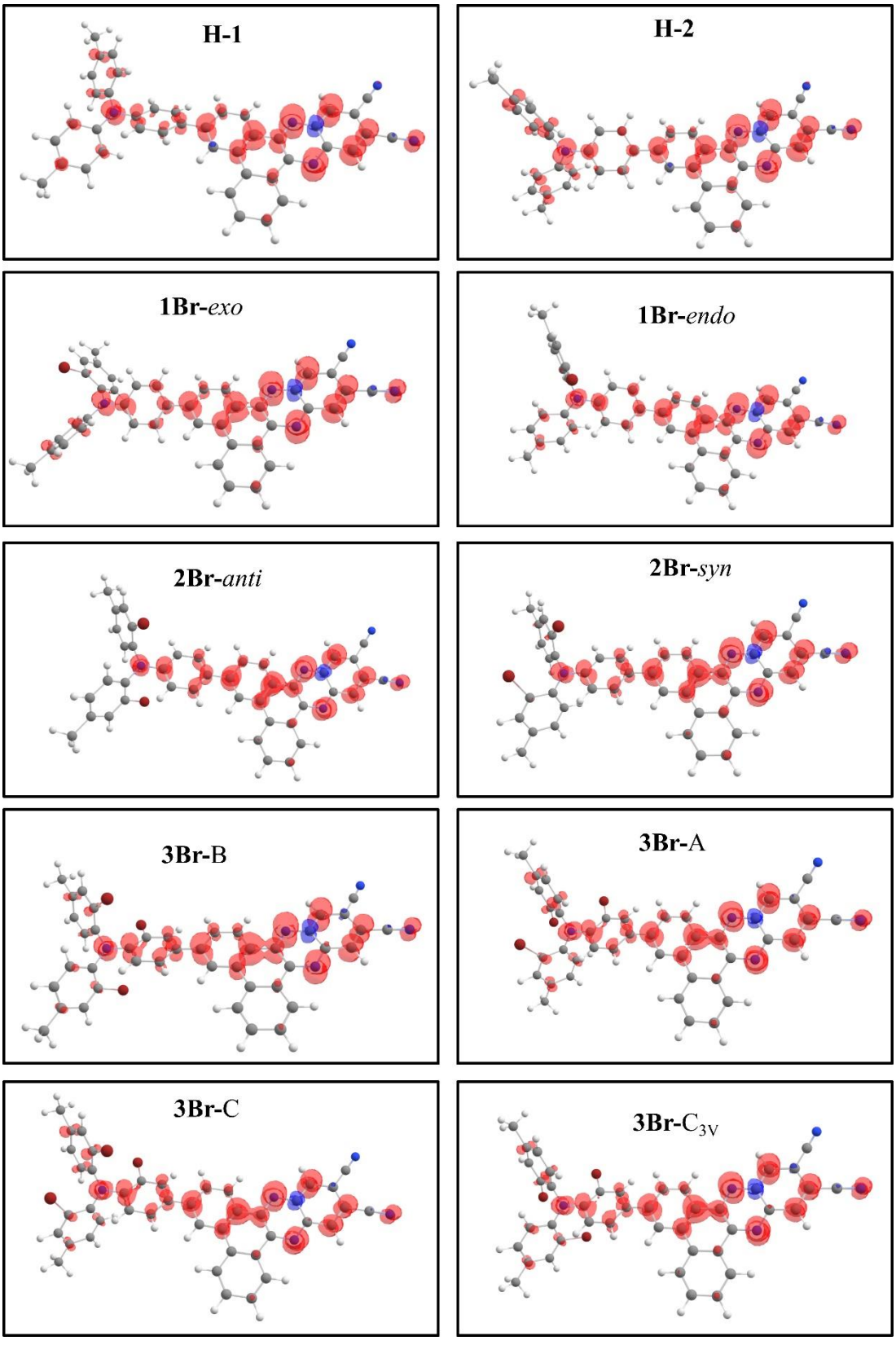

Figure S10. Triplet spin density distribution (TSDD) maps

Section S3: NMR spectra of target emitters

^{1}H NMR spectrum of 3-(4-((2-bromo-4-methylphenyl)(*p*-tolyl)amino)phenyl)-dibenzo[*a*,*c*] phenazine-11,12-dicarbonitrile (**1Br**) in $CDCl_3$

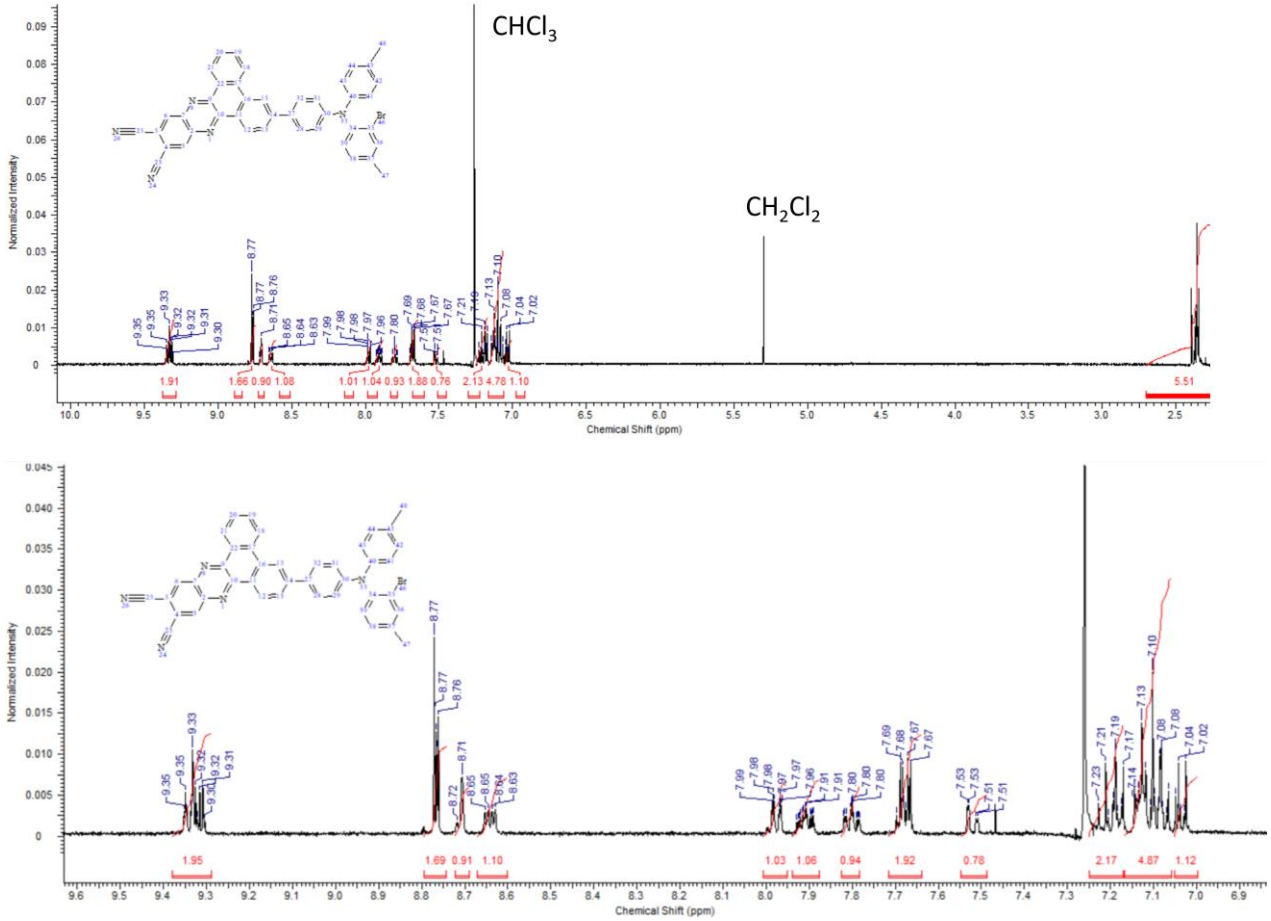

^{1}H NMR spectrum of 3-(4-(bis(2-bromo-4-methylphenyl)amino)phenyl)dibenzo[*a*,*c*] phenazine-11,12-dicarbonitrile (**2Br**) in $CDCl_3$.

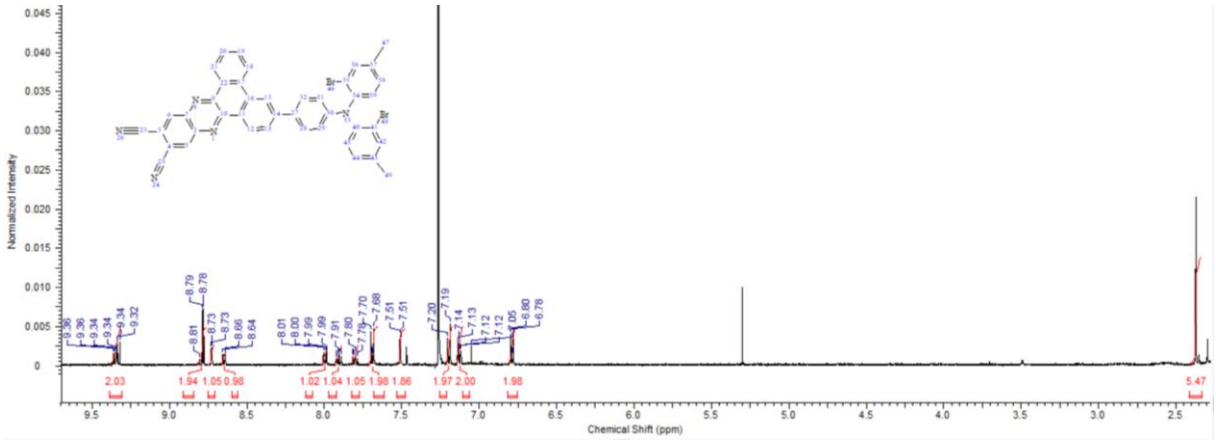

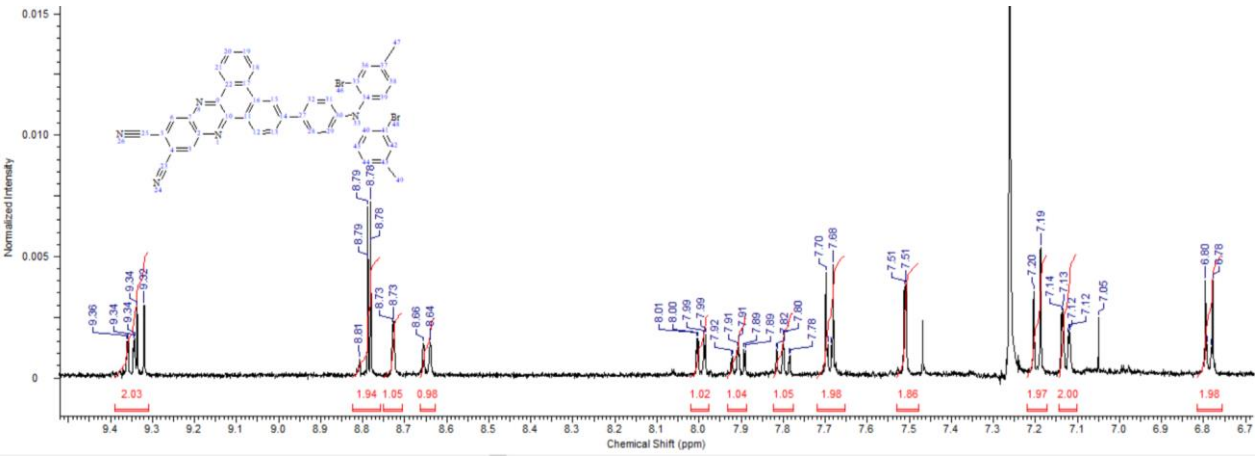

^{1}H NMR spectrum of 3-(4-(bis(2-bromo-4-methylphenyl)amino)phenyl)dibenzo [*a*,*c*]phenazine-11,12-dicarbonitrile (**3Br**) in $CDCl_3$.

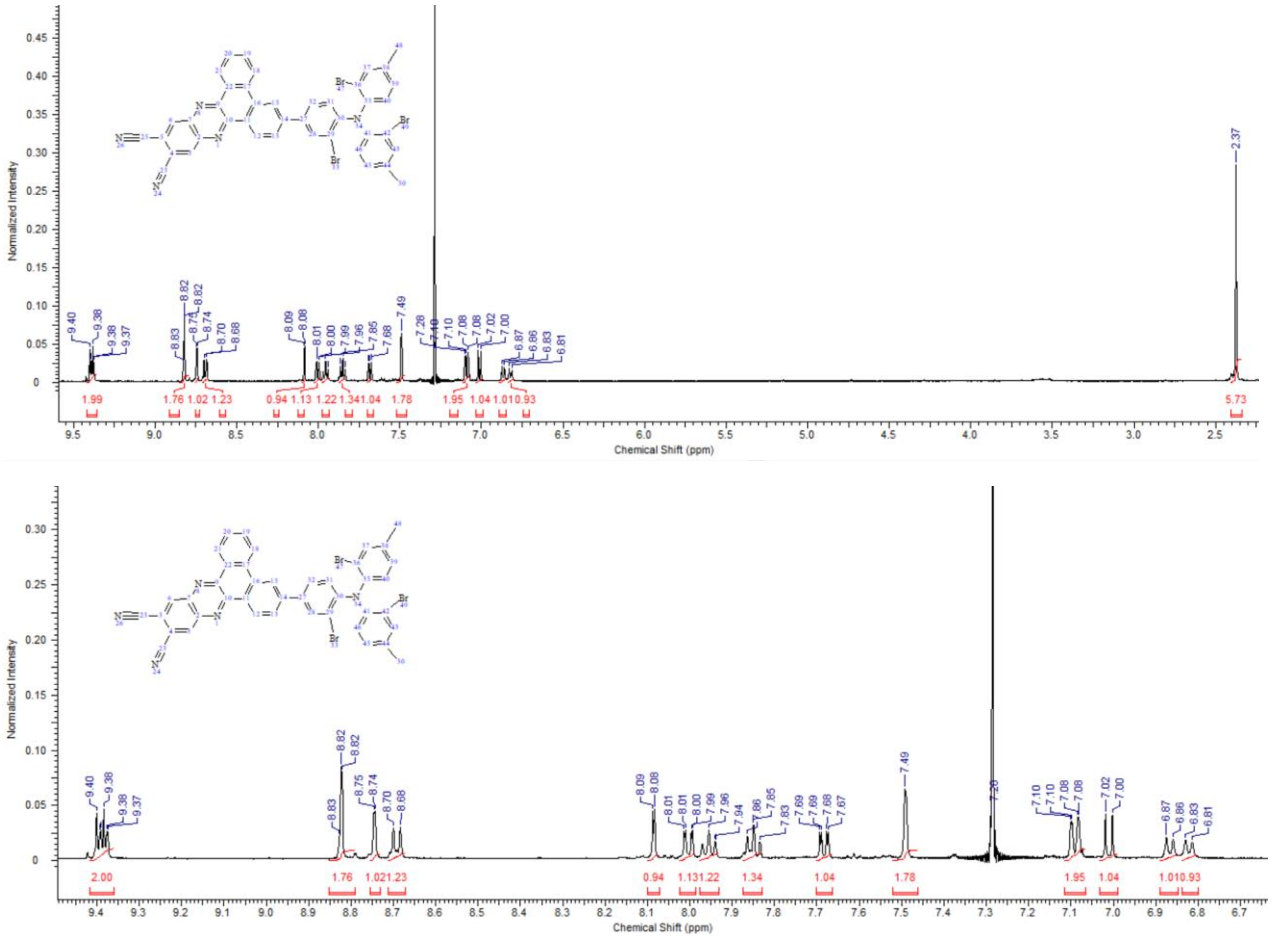

^{1}H NMR spectrum of 3-(4-(bis(2-bromo-4-methylphenyl)amino)phenyl)phenanthrene-9,10-dione (**2**) in $CDCl_3$.

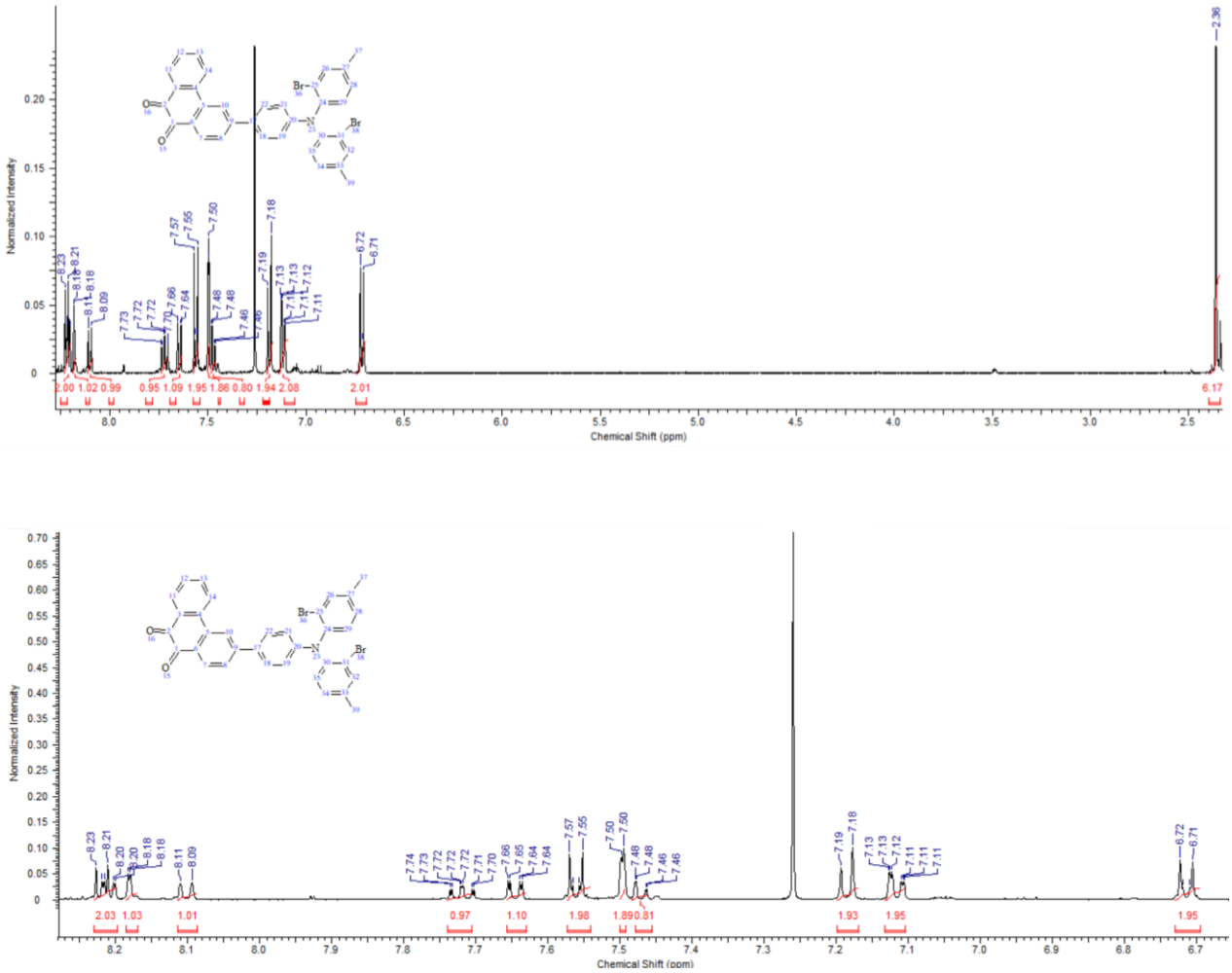

^{1}H NMR spectrum of 3-(4-(bis(2-bromo-4-methylphenyl)amino)-3-bromophenyl)-phenanthrene-9,10-dione (**3**) in $CDCl_3$

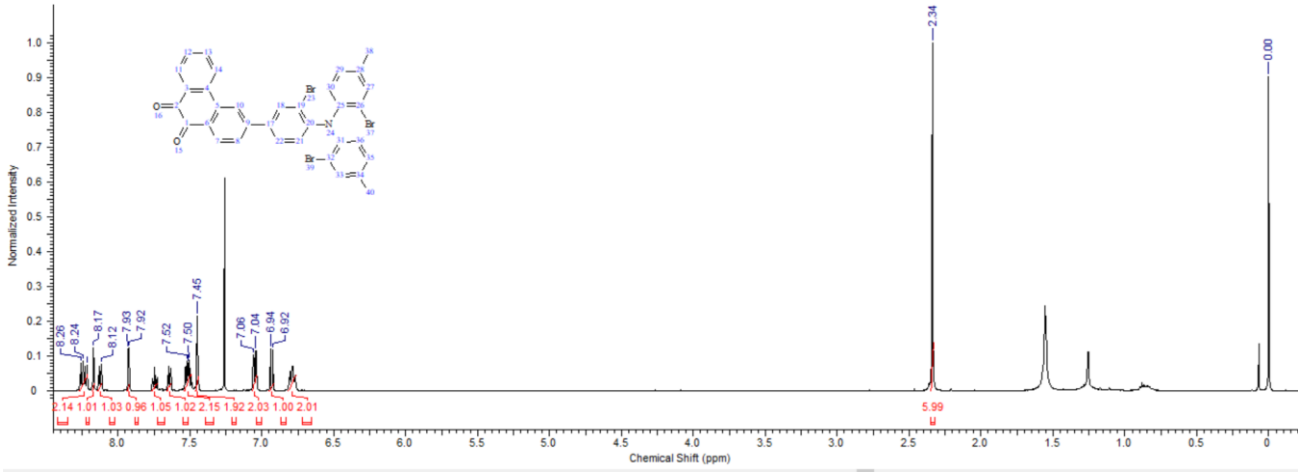

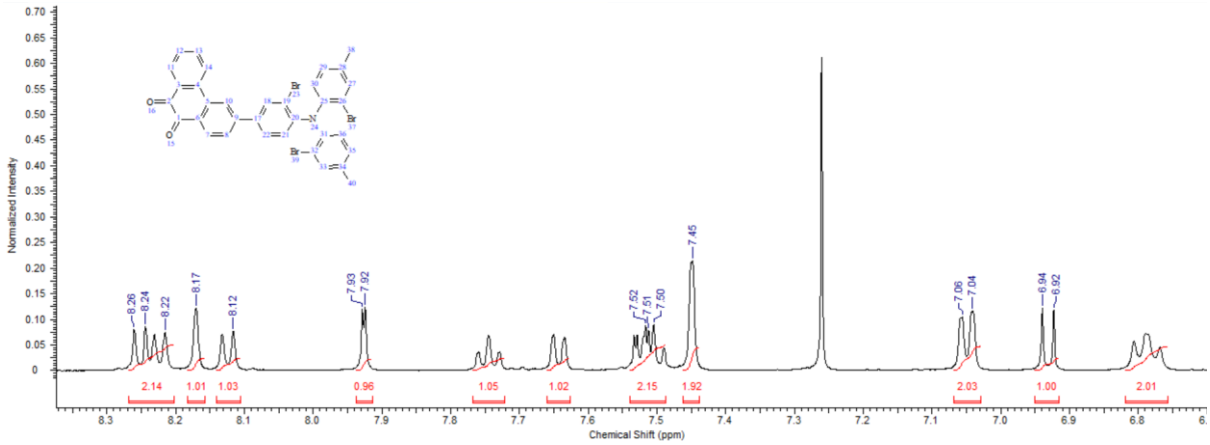

Section S4: Determination of photophysical parameters

PL decay curves (presented in **Figures 2F** and **S4**) were fitted with the multiexponential equation:

$$I(t) = A_0 + \sum_{i=1}^{n} A_i \exp\left(-{}^{t}/_{\tau_i}\right) \quad \text{(S6)}$$

where A_i is the pre-exponential factor, τ_i is the decay time and $I(t)$ is emission intensity. Average lifetimes of prompt (τ_{PF}) and delayed fluorescence (τ_{DF}) were determined using the following formula:

$$\tau_{PF}, \tau_{DF} = \sum_{i=1}^{n} f_i \tau_i, \quad \text{(S7)}$$

where $f_i$is fractional contribution of i-th component expressed as:

$$f_i = \frac{A_i \tau_i}{\sum_{i=1}^{n} A_i \tau_i} \quad \text{(S8)}$$

The ratio of DF and PF quantum yields $\varphi_{DF}/\varphi_{PF}$ was determined as follows:

$$\frac{\varphi_{DF}}{\varphi_{PF}} = \frac{\sum_{i=1}^{n} \tau_{DF(i)} A_{DF(i)}}{\sum_{j=1}^{n} \tau_{PF(j)} A_{PF(j)}} \quad \text{(S9)}$$

where $A_{DF(i)}$ and $A_{PF(j)}$ is the pre-exponential factor of delayed and prompt fluorescence component, respectively; $\tau_{DF(i)}$and $\tau_{PF(j)}$ is the lifetime of delayed and prompt fluorescence component, respectively. The rate constants of radiative (k_r) and nonradiative (k_{nr}) decay and intersystem crossing (k_{ISC}) are given by equations[S2]:

$$k_r = \frac{\varphi_{PF}}{\tau_{PF}}, \quad \text{(S10)}$$

$$k_{ISC} = \frac{\varphi_{DF}}{\varphi\, \tau_{PF}}, \quad \text{(S11)}$$

$$k_{nr} = \frac{1}{\tau_{PF}} - (k_r + k_{ISC}). \quad \text{(S12)}$$

*w*here φ is PLQY ($\varphi_{DF} + \varphi_{PF}$). Further, the quantum yields for ISC and rISC were calculated as

$$\varphi_{ISC} = k_{ISC} \tau_{PF}, \quad \text{(S13)}$$

$$\varphi_{rISC} = \frac{1 - \varphi_{PF}/\varphi}{\varphi_{ISC}}. \quad \text{(S14)}$$

Finally, the rate constant of rISC (k_{rISC}) was calculated as

$$k_{rISC} = \frac{\varphi_{rISC}}{\tau_{DF}}\left(\frac{\varphi}{\varphi_{PF}}\right). \quad \text{(S15)}$$

Thus obtained photophysical parameters are presented in **Table 2** (main text).

References

[S1] M. Mońka, I. E. Serdiuk, K. Kozakiewicz, E. Hoffman, J. Szumilas, A. Kubicki, S. Y. Park and P. Bojarski, *Mater. Chem. C*. 2022, **10**, 7925-7934.

[S2] Tao, Y.; Yuan, K.; Chen, T.; Xu, P.; Li, H.; Chen, R.; Zheng, C.; Zhang, L.; Huang, W. Thermally Activated Delayed Fluorescence Materials Towards the Breakthrough of Organoelectronics. *Adv. Mater*. **2015**, *26*, 7931 – 7958.